Available online at www.sciencedirect.com
ScienceDirect
Journal of Sound and Vibration 300 (2007) 316–329
JOURNAL OF SOUND AND VIBRATION
www.elsevier.com/locate/jsvi

Computing the dynamic response of an axially moving continuum

Gregor Čepon, Miha Boltežar*

Faculty of Mechanical Engineering, University of Ljubljana, Aškerčeva 6, 1000 Ljubljana, SI-Slovenia

Received 21 December 2005; received in revised form 17 July 2006; accepted 10 August 2006
Available online 9 October 2006

Abstract

The aim of this study was to apply an approximate Galerkin finite-element method to solve the initial boundary-value problem of a viscously damped axially moving pre-tensioned beam including arbitrary support excitations. In order to validate the Galerkin finite-element method the results were compared with exact solutions when available and with solutions obtained using the finite-difference and Galerkin methods. The energy dissipation of the system was considered in the form of an equivalent viscous-damping model. It was also shown that for certain values of the parameters, especially at high velocities, the Galerkin method using stationary string eigenfunctions can give a poor prediction of the dynamic response.

1. Introduction

Many engineering devices can be represented by axially moving systems, for example, power-transmission belts, plastic films, chain drives, magnetic tapes, paper sheets and textile fibers. To ensure that such structural systems operate under stable working conditions, the dynamic response and stability of such systems have been studied extensively. A great deal of research has been done on the transverse vibrations of such systems. The traveling flexible string and the traveling, tensioned Euler–Bernoulli beam are the most common models of axially moving continua. The early research in this area includes studies by Mahalingam [1] and Archibald and Emslie [2] who started to investigate the transverse oscillations of traveling string. The literature regarding axially moving systems is extensive, in Ref. [3] a thorough literature review up to 1992 can be found. Among the studies reviewed in Ref. [3] there are several investigations considering the vibrations of a belt moving with time-dependent velocity [4–6]. A stability analysis was preformed, assuming that time-dependent velocity is varying harmonically. Later, Chen and Yang [7] investigated the transverse vibrations of a viscoelastic beam with time-dependent speed. The fundamental role of nonlinearity has been widely studied in Refs. [8–12]. Al-Jawi [13–15] first investigated the vibration localization phenomenon in dual-span axially moving beams.

While for more accurate results, a nonlinear model is required, in this paper a simple linear model of an axially moving beam, taking into account support excitation, was proposed. To the authors' surprise the

*Corresponding author. Tel.: + 386 1 4771 608; fax: +386 1 2518 567.
E-mail address: miha.boltezar@fs.uni-lj.si (M. Boltežar).

doi:10.1016/j.jsv.2006.08.014

literature that deals with the transverse oscillation of an axially moving continuum due to the lateral vibrations of supports is limited. In two classic articles [1,2] the transverse oscillations of a traveling string due to the sinusoidal lateral vibrations of the supports was investigated. Wickert and Mote [16] determined the response of an axially moving string and beam to arbitrary excitations and the initial conditions using two closed-form solutions: a modal analysis and a Green's function method. These techniques were also applied to an axially moving beam that is excited by a prescribed transverse support motion. Recently, Horssen published a paper [17] where the axially moving string problem was solved exactly using the standard method of Laplace transforms. An analytical solution was derived for arbitrary lateral vibrations of the supports. In general, analytical solutions for the vibrations of axially moving continua are difficult to find. Pramila [18] proposed a finite-element method (FEM) for a moving beam on an elastic foundation. In this work, the boundary conditions do not include support excitations. In all of these studies [1,2,8,17,18] the axially moving one-dimensional structures were assumed to be elastic. Thus, in this work the dissipation of energy was considered in the form of an equivalent viscous-damping model, see also Ref. [19]. An approximate Galerkin finite-element method was applied to solve the initial boundary-value problem of a viscously damped, axially moving pre-tensioned beam, including arbitrary support excitations. Although the Galerkin finite-element method is widely used, to the best of authors' knowledge it has not yet been applied to the problem analyzed in this paper. In order to validate the Galerkin finite-element method the results were compared with the result obtained using the finite-difference and Galerkin methods. When possible the approximate solutions were also compared with the exact solutions given in Ref. [17]. The Galerkin method is widely used in the literature [4,10,13–15,20,21] for the spatial discretization of an axially moving continuum. When using the Galerkin method the transverse displacement field is usually expanded into a sine series, which represents the eigenfunctions of a simply supported stationary string. Rajesh and Parker [22] have examined the spatial discretization of the eigenvalue problems of axially moving continua from the perspectives of a moving versus a stationary basic-functions system. They stated that a stationary system's basic functions are the most reliable basic functions when the aim is to obtain the natural frequencies and the mode shapes at subcritical velocities. From the results presented in this work it is obvious that this is not the case when the interest lies in obtaining the dynamic response. In numerical examples, we have shown that for certain values of the parameters, especially at high velocities, the Galerkin method seems to give a poor prediction of the dynamic response. Although the Galerkin method is widely used, no such phenomenon has been reported in the literature. Moreover, the proposed Galerkin finite-element method gives a good prediction of the dynamic response for various parameters of the system.

This paper is organized as follows. First, in Section 2, the equation of the axially moving beam is given. The spatial discretization of the problem using the Galerkin finite-element method is presented in Section 3; this section also presents the algorithm for the Galerkin and Newmark methods. In Section 4, the algorithm for the finite-difference method is briefly presented. The numerical results are presented in Section 5, and the conclusions are drawn in Section 6.

2. Equation of motion

Consider a belt moving with an axial velocity between two supports that are a distance L apart, as shown in Fig. 1. The transverse vibrations of the belt can be modeled as a moving beam. The mathematical model of a moving beam is based on the following assumptions:

- the tension in the beam is constant,
- the lateral vibrations are small,

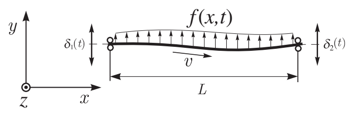

Fig. 1. Moving belt between two supports.

- the effect of gravity is neglected,
- the effect of air drag is taken into consideration,
- the mass of the beam per unit length is constant,
- the axial velocity of the beam is constant.

Using these assumptions the equation of motion can be written in the form

$$a^2 \frac{\partial^4 w(x,t)}{\partial x^4} - (c^2 - v^2) \frac{\partial^2 w(x,t)}{\partial x^2} + 2v \frac{\partial^2 w(x,t)}{\partial x \, \partial t} + \frac{\partial^2 w(x,t)}{\partial t^2} + b \frac{\partial w(x,t)}{\partial t} + bv \frac{\partial w(x,t)}{\partial x} = \frac{1}{m} f(x,t), \quad (1)$$

where

$$a = \sqrt{\frac{EI}{m}}, \quad c = \sqrt{\frac{T}{m}}, \quad b = \frac{d}{m}.$$

The variable $w(x,t)$ denotes the transverse displacement, E is the Young's modulus, I is the moment of inertia of the beam's cross-section about the z-axis, T is the axial tension force, $f(x,t)$ is the distributed load, v is the axial velocity, and d is the viscous-damping coefficient. When the bending stiffness in Eq. (1) is omitted, $a = 0$, the equation of an axially moving viscously damped string is obtained. If the belt drive runs at a constant velocity the eccentricity of the pulleys gives both ends of the belt span transverse displacements like those shown in Fig. 1. Pulley eccentricity can also cause periodic tension variations in the belt span [23]. In our case we have neglected this effect. Considering the fundamental components of these excitations, the boundary conditions for Eq. (1) can be written as

$$w(0,t) = \delta_1(t), \quad w(L,t) = \delta_2(t), \quad (2)$$

$$\frac{\partial^2}{\partial x^2} w(0,t) = 0, \quad \frac{\partial^2}{\partial x^2} w(L,t) = 0, \quad (3)$$

where $\delta_1(t)$ and $\delta_2(t)$ represent the functions of the generalized support excitations. The initial deflection and the initial velocity of the deflection are expressed as

$$w(x,0) = h(x) \quad \text{and} \quad \frac{\partial w(x,0)}{\partial t} = g(x). \quad (4)$$

3. Solution methods

The equation of motion (1) has to be modified before the approximate Galerkin finite-element method can be applied. Taking into consideration the prescribed displacement of the supports, the total response of the linear beam model can be obtained from the principle of superposition. The basic step in the formulation of the problem is to express the displacement response of the beam as the sum of the displacements that would be induced by the support motion applied statically (the so-called pseudo-static displacement $w_s(x,t)$) together with the additional displacement due to the dynamic effects $w_d(x,t)$, as shown in Fig. 2.

$$w(x,t) = w_s(x,t) + w_d(x,t). \quad (5)$$

Substituting Eq. (5) into Eq. (1) we get

$$a^2 \frac{\partial^4 w_d(x,t)}{\partial x^4} - (c^2 - v^2) \frac{\partial^2 w_d(x,t)}{\partial x^2} + 2v \frac{\partial^2 w_d(x,t)}{\partial x \, \partial t} + \frac{\partial^2 w_d(x,t)}{\partial t^2} + b \frac{\partial w_d(x,t)}{\partial t} + bv \frac{\partial w_d(x,t)}{\partial x} = \frac{1}{m} f(x,t) + p_{\text{eff}}(x,t) \quad (6)$$

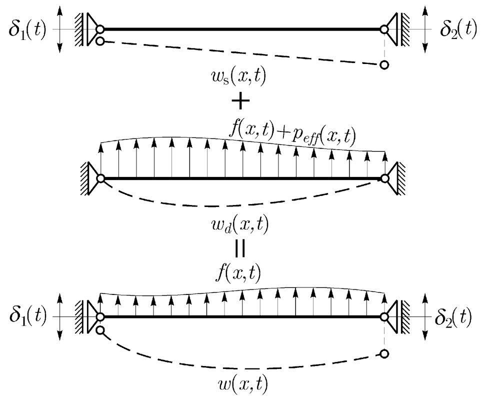

Fig. 2. Deflection of the beam as the sum of the pseudo-static and dynamic deflections.

where

$$p_{\mathrm{eff}}(x,t) = -a^2\frac{\partial^4 w_s(x,t)}{\partial x^4} + (c^2 - v^2)\frac{\partial^2 w_s(x,t)}{\partial x^2} - 2v\frac{\partial^2 w_s(x,t)}{\partial x\,\partial t} - \frac{\partial^2 w_s(x,t)}{\partial t^2} - b\frac{\partial w_s(x,t)}{\partial t} - bv\frac{\partial w_s(x,t)}{\partial x} \tag{7}$$

represents the effective load applied to the beam segment by the support excitations. The pseudo-static displacement $w_s(x,t)$ in Eq. (7) can be written as

$$w_s(x,t) = \delta_1(t)\left(1 - \frac{x}{L}\right) + \delta_2(t)\frac{x}{L} = \sum_{j=1}^{2}\delta_j(t)\varphi_j(x), \tag{8}$$

where $\varphi_j(x)$ represents the displacement shapes. Substituting Eq. (8) into Eq. (7) leads to an expression for the effective load

$$p_{\mathrm{eff}}(x,t) = -\sum_{j=1}^{2}\left((2v\dot{\delta}_j(t) + bv\delta_j(t))\frac{\mathrm{d}\varphi_j(x)}{\mathrm{d}x} + (\ddot{\delta}_j(t) + b\dot{\delta}_j(t))\varphi_j(x)\right). \tag{9}$$

Substituting Eq. (9) into Eq. (6) we get

$$a^2\frac{\partial^4 w_d(x,t)}{\partial x^4} - (c^2 - v^2)\frac{\partial^2 w_d(x,t)}{\partial x^2} + 2v\frac{\partial^2 w_d(x,t)}{\partial x\,\partial t} + \frac{\partial^2 w_d(x,t)}{\partial t^2} + b\frac{\partial w_d^k(x,t)}{\partial t} + bv\frac{\partial w_d^k(x,t)}{\partial x} = \frac{1}{m}f(x,t) - \sum_{j=1}^{2}\left((2v\dot{\delta}_j(t) + bv\delta_j(t))\frac{\mathrm{d}\varphi_j(x)}{\mathrm{d}x} + (\ddot{\delta}_j(t) + b\dot{\delta}_j(t))\varphi_j(x)\right). \tag{10}$$

The boundary conditions expressing the displacement for Eq. (10) can be written in the form

$$w_d(0,t) = 0, \quad w_d(L,t) = 0. \tag{11}$$

On the other hand, the boundary conditions (3) remain the same.

3.1. Spatial discretization using the approximate Galerkin finite-element method

The spatial discretization of Eq. (10) is done using the Galerkin finite-element method. By multiplying Eq. (10) by a weight function $u(x)$ and by integrating over the domain $x \in [0, L]$

we obtain [24]

$$\int_0^L \Bigg(a^2 \frac{\partial^4 w_d(x,t)}{\partial x^4} - (c^2 - v^2) \frac{\partial^2 w_d(x,t)}{\partial x^2} + 2v \frac{\partial^2 w_d(x,t)}{\partial x \, \partial t} + \frac{\partial^2 w_d(x,t)}{\partial t^2} + b \frac{\partial w_d(x,t)}{\partial t} + bv \frac{\partial w_d(x,t)}{\partial x}$$
$$- \frac{1}{m} f(x,t) + \sum_{j=1}^{2} \Big((2v\dot{\delta}_j(t) + bv\delta_j(t)) \frac{\mathrm{d}\varphi_j(x)}{\mathrm{d}x} + (\ddot{\delta}_j(t) + b\dot{\delta}_j(t))\varphi_j(x) \Big) \Bigg) u(x)\,\mathrm{d}x = 0. \tag{12}$$

Eq. (12) is referred to as a variational form of Eq. (10). Mathematically, it will be assumed that $u(x)$ is continuously differentiable in the interval $x \in [0, L]$. By integrating the fourth derivative term by parts, Eq. (12) can be expressed as

$$a^2 \int_0^L \left(\frac{\partial^2 w_d(x,t)}{\partial x^2} \frac{\mathrm{d}^2 u(x)}{\mathrm{d}x^2} \right) \mathrm{d}x - (c^2 - v^2) \int_0^L \left(\frac{\partial^2 w_d(x,t)}{\partial x^2} u(x) \right) \mathrm{d}x + 2v \int_0^L \left(\frac{\partial^2 w_d(x,t)}{\partial x \, \partial t} u(x) \right) \mathrm{d}x$$
$$+ \int_0^L \left(\frac{\partial^2 w_d(x,t)}{\partial t^2} u(x) \right) \mathrm{d}x + b \int_0^L \left(\frac{\partial w_d(x,t)}{\partial t} u(x) \right) \mathrm{d}x + bv \int_0^L \left(\frac{\partial w_d(x,t)}{\partial x} u(x) \right) \mathrm{d}x$$
$$= \frac{1}{m} \int_0^L f(x,t) u(x)\,\mathrm{d}x - \sum_{j=1}^{2} (2v\dot{\delta}_j(t) + bv\delta_j(t)) \int_0^L \frac{\mathrm{d}\varphi_j(x)}{\mathrm{d}x} u(x)\,\mathrm{d}x$$
$$- \sum_{j=1}^{2} (\ddot{\delta}_j(t) + b\dot{\delta}_j(t)) \int_0^L \varphi_j(x) u(x)\,\mathrm{d}x - \frac{1}{m} [T(x)u(x)]_0^L + \frac{1}{m} \left[M(x) \frac{\partial u(x)}{\partial x} \right]_0^L, \tag{13}$$

which is the so-called weak form of Eq. (12). The variables $T(x)$ and $M(x)$ denote the shear force and the bending moment. The approximate solution on the subinterval $x \in [x_{e-1}, x_e]$ of length h, can be written as

$$w_d^e(x,t) = \sum_{j=1}^{4} U_j^e(t) \psi_j^e(x) \tag{14}$$

where U_1^e and U_2^e denote the deflection and rotation of the nodal point at the left-hand end of the finite element. The variables U_3^e and U_4^e denote the deflection and rotation at the right-hand end of the finite element. The third-order Hermite polynomials ψ_1^e, ψ_2^e, ψ_3^e and ψ_4^e are given by the equations

$$\psi_1^e(x) = \left(2 \frac{x - x_{e-1}}{h} + 1 \right) \left(\frac{x - x_{e-1}}{h} - 1 \right)^2, \quad \psi_2^e(x) = \frac{x - x_{e-1}}{h} \left(1 - \frac{x - x_{e-1}}{h} \right)^2 h, \tag{15}$$

$$\psi_3^e(x) = \left(\frac{x - x_{e-1}}{h} \right)^2 \left(3 - 2 \frac{x - x_{e-1}}{h} \right), \quad \psi_4^e(x) = \left(\frac{x - x_{e-1}}{h} \right)^2 \left(\frac{x - x_{e-1}}{h} - 1 \right) h. \tag{16}$$

Replacing $w_d(x,t)$ in Eq. (13) with the approximation given by Eq. (14), we obtain

$$\sum_{j=1}^{4} \ddot{U}_j^e(t) \underbrace{\int_{x_{e-1}}^{x_e} \psi_j^e(x) \psi_i^e(x)\,\mathrm{d}x}_{M_{ij}^e} + \sum_{j=1}^{4} \dot{U}_j^e(t) \underbrace{\left(2v \int_{x_{e-1}}^{x_e} \frac{\mathrm{d}\psi_j^e(x)}{\mathrm{d}x} \psi_i^e(x)\,\mathrm{d}x + b \int_{x_{e-1}}^{x_e} \psi_j^e(x) \psi_i^e(x)\,\mathrm{d}x \right)}_{C_{ij}^e}$$
$$+ \sum_{j=1}^{4} U_j^e(t) \underbrace{\left(a^2 \int_{x_{e-1}}^{x_e} \frac{\mathrm{d}^2\psi_j^e(x)}{\mathrm{d}x^2} \frac{\mathrm{d}^2\psi_i^e(x)}{\mathrm{d}x^2}\,\mathrm{d}x - (c^2 - v^2) \int_{x_{e-1}}^{x_e} \frac{\mathrm{d}^2\psi_j^e(x)}{\mathrm{d}x^2} \psi_i^e(x)\,\mathrm{d}x + bv \int_{x_{e-1}}^{x_e} \frac{\mathrm{d}\psi_j^e(x)}{\mathrm{d}x} \psi_i^e(x)\,\mathrm{d}x \right)}_{K_{ij}^e}$$
$$= \underbrace{\frac{1}{m} \int_{x_{e-1}}^{x_e} f(x,t) \psi_i^e(x)\,\mathrm{d}x}_{F_i^e} - \underbrace{\sum_{j=1}^{2} (2v\dot{\delta}_j(t) + bv\delta_j(t)) \int_{x_{e-1}}^{x_e} \frac{\mathrm{d}\varphi_j(x)}{\mathrm{d}x} \psi_i^e(x)\,\mathrm{d}x}_{\gamma_i^e}$$

$$-\underbrace{\sum_{j=1}^{2}(\ddot{\delta}_j(t)+b\dot{\delta}_j(t))\int_{x_{e-1}}^{x_e}\varphi_j(x)\psi_i^e(x)\,\mathrm{d}x}_{\phi_i^e}-\underbrace{\frac{1}{m}[T(x)\psi_i^e(x)]_{x_{e-1}}^{x_e}+\frac{1}{m}\left[M(x)\,\frac{\mathrm{d}\psi_i^e(x)}{\mathrm{d}x}\right]_{x_{e-1}}^{x_e}}_{P_i^e},\quad i=1,2,3,4. \tag{17}$$

By using Simpson's approximate formula for solving integrals, the variables F_i^e and ϕ_i^e can be written as:

$$F_1^e=\frac{1}{6}\frac{h}{m}(2f(x_{e-1},t)+f(x_e,t)),\quad F_2^e=\frac{1}{24}\frac{h^2}{m}(f(x_{e-1},t)+f(x_e,t)),$$
$$F_3^e=\frac{1}{6}\frac{h}{m}(f(x_{e-1},t)+2f(x_e,t)),\quad F_4^e=-\frac{1}{24}\frac{h^2}{m}(f(x_{e-1},t)+f(x_e,t)),$$

$$\phi_1^e=\sum_{j=1}^{2}(\ddot{\delta}_j(t)+b\dot{\delta}_j(t))\,\frac{h}{6}(2\varphi_j(x_{e-1})+\varphi_j(x_e)),$$
$$\phi_2^e=\sum_{j=1}^{2}(\ddot{\delta}_j(t)+b\dot{\delta}_j(t))\,\frac{h^2}{24}(\varphi_j(x_{e-1})+\varphi_j(x_e)),$$
$$\phi_3^e=\sum_{j=1}^{2}(\ddot{\delta}_j(t)+b\dot{\delta}_j(t))\,\frac{h}{6}(\varphi_j(x_{e-1})+2\varphi_j(x_e)),$$
$$\phi_4^e=-\sum_{j=1}^{2}(\ddot{\delta}_j(t)+b\dot{\delta}_j(t))\,\frac{h^2}{24}(\varphi_j(x_{e-1})+\varphi_j(x_e)).$$

The integrals in expression (17) relating to the variables γ_i^e can be solved analytically:

$$\gamma_1^e=\gamma_3^e=\frac{hv}{2L}(2(\dot{\delta}_2(t)-\dot{\delta}_1(t))+b(\delta_2(t)-\delta_1(t))), \tag{18}$$
$$\gamma_2^e=-\gamma_4^e=\frac{h^2v}{12L}(2(\dot{\delta}_2(t)-\dot{\delta}_1(t))+b(\delta_2(t)-\delta_1(t))). \tag{19}$$

The moment and shear force at the left- and right-hand nodal points of the finite element are given by the variable P_i^e:

$$P_1^e=\frac{1}{m}\,T_e(x_{e-1}),\quad P_2^e=-\frac{1}{m}\,M_e(x_{e-1}),\quad P_3^e=-\frac{1}{m}\,T_e(x_e),\quad P_4^e=\frac{1}{m}\,M_e(x_e). \tag{20}$$

Thus, the equation of the finite element can be written as a set of linear differential equations of the second order

$$\mathbf{M_e}\ddot{\mathbf{u}}_\mathbf{e}(t)+\mathbf{C_e}\dot{\mathbf{u}}_\mathbf{e}(t)+\mathbf{K_e}\mathbf{u_e}(t)=\mathbf{f_e}(t)+\mathbf{p}_e(t). \tag{21}$$

The elements of the mass $\mathbf{M_e}$, the damping $\mathbf{C_e}$ and the stiffness $\mathbf{K_e}$ matrix of the finite element are given in Appendix A. The forcing vector $\mathbf{f_e}(t)$ and the vector $\mathbf{p_e}(t)$ with the nodal values of the shear forces and the bending moments have the following form:

$$\mathbf{f_e}(t)=\begin{Bmatrix}F_1^e\\F_2^e\\F_3^e\\F_4^e\end{Bmatrix}-\begin{Bmatrix}\phi_1^e\\\phi_2^e\\\phi_3^e\\\phi_4^e\end{Bmatrix}-\begin{Bmatrix}\gamma_1^e\\\gamma_2^e\\\gamma_3^e\\\gamma_4^e\end{Bmatrix};\quad \mathbf{p}_e(t)=\begin{Bmatrix}P_1^e\\P_2^e\\P_3^e\\P_4^e\end{Bmatrix}.$$

The deflections and rotations of the nodal points of the finite element are given in the vector $\mathbf{u_e}(t)=\{U_1^e, U_2^e, U_3^e, U_4^e\}^\mathrm{T}$. The next step in the process is the summation over the elements, as shown in Fig. 3. The first and penultimate equations have to be removed, because of the boundary conditions (11) that prescribe the zero deflection of the nodal points $U_1(t)=0$ and $U_{2n+1}(t)=0$. The reduced equation of the

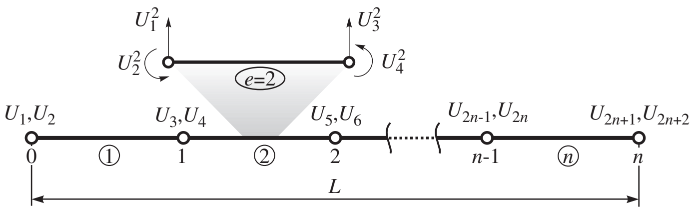

Fig. 3. Summation over the finite elements.

problem can be written as

$$\mathbf{M}\ddot{\mathbf{u}}(t) + \mathbf{C}\dot{\mathbf{u}}(t) + \mathbf{K}\mathbf{u}(t) = \underbrace{\mathbf{f}(t) + \mathbf{p}(t)}_{\mathbf{F}(t)}, \tag{22}$$

where **M** is the mass matrix, **C** is the damping matrix and **K** is the stiffness matrix of size $2n \times 2n$, where n denotes the number of finite elements (Fig. 3). Regarding the boundary conditions, and assuming that no external forces and moments act on the beam along its length, the vector $\mathbf{p}(t)$ can be written as

$$\mathbf{p}(t) = \{0, 0, \ldots, 0\}^{\mathrm{T}}. \tag{23}$$

3.2. Spatial discretization using the Galerkin method

In this section the Galerkin method is applied to solve Eq. (10). The trial function is chosen to be in the form,

$$w(x,t) = \sum_{i=1}^{N} q_i(t) \sin\left(\frac{i\pi x}{L}\right), \tag{24}$$

where $\sin(i\pi x/L)$ is the ith eigenfunction of a simply supported stationary string, and $q_i(t)$ are generalized displacements. The variable N denotes the number of terms in the series solution. The application of Galerkin's method provides a set of ordinary differential equations in the form

$$\mathbf{M}\ddot{\mathbf{q}}(t) + \mathbf{C}\dot{\mathbf{q}}(t) + \mathbf{K}\mathbf{q}(t) = \mathbf{F}(t), \tag{25}$$

where **M**, **C** and **K** are the mass, damping and stiffness matrices.

3.3. Time discretization using the Newmark method

The Newmark scheme is a classic time-stepping algorithm, popular in structural mechanics [24]. Before applying the method to the system of Eqs. (22) or (25), they have to be rewritten in the form

$$\ddot{\mathbf{u}}(t) = \mathbf{g}(t, \mathbf{u}(t), \dot{\mathbf{u}}(t))) = \mathbf{M}^{-1}(\mathbf{F}(t) - \mathbf{C}\dot{\mathbf{u}}(t) - \mathbf{K}\mathbf{u}(t)). \tag{26}$$

Using the Newmark method the dynamic response of the system is obtained. From this point on the Galerkin-finite-element-Newmark (GFEN) method will denote the method where the spatial discretization of the initial boundary-value problem (1)–(4) is made using the Galerkin finite-element method, and time discretization of the problem is made using the Newmark method. Similarly, the Galerkin–Newmark (GN) method will denote the method where the spatial discretization of the initial boundary-value problem (1)–(4) is made using the Galerkin method and the time discretization of the problem is made using the Newmark method.

4. Central finite-difference approximation of the axially moving beam equation

The central difference method will be used to find an approximate solution of the initial boundary-value problem (1)–(4) [24]. Finite-difference methods provide a powerful approach to solving differential equations and are widely used in many fields of applied sciences. The function $w(x,t)$ depends on two variables, $x \in [0, L]$

and $t \in [0, t_k]$. A discretization of the function $w(x, t)$ is obtained by considering only the values $w_i^k = w(x_i, t_k)$ at a finite number of points $(ih, k\Delta t)$. The central finite-difference approximations of the derivatives are given in Appendix B. Applying the boundary conditions given with Eqs. (2) and (3), the nodal values w_{-1}^k, w_0^k, w_n^k and w_{n+1}^k can be expressed as

$$w_0^k = \delta_1(t_k), \quad w_n^k = \delta_2(t_k), \quad t > 0, \tag{27}$$

$$w_{-1}^k = 2w_0^k - w_1^k, \quad w_{n+1}^k = 2w_n^k - w_{n-1}^k, \quad t > 0. \tag{28}$$

By using the approximations given with Eqs. (35)–(40) and considering the boundary conditions (27) and (28), Eq. (1) can be written as a set of $n - 1$ linear equations

$$\mathbf{A}_M \mathbf{w}^{k+1} = \mathbf{A}_K \mathbf{w}^k + \mathbf{A}_C \mathbf{w}^{k-1} + \mathbf{f}^k, \quad k = 0, 1, 2, \ldots, \tag{29}$$

where $\mathbf{w}^k = \{w_1^k, w_2^k, \ldots, w_{n-1}^k\}^{\mathrm{T}}$ and $\mathbf{f}^k = \{f(x_1, t_k), f(x_2, t_k), \ldots, f(x_{n-1}, t_k)\}^{\mathrm{T}}$. In the first integration step the $k = 0$ initial conditions (4) have to be taken into consideration

$$\mathbf{w}^{-1} = \mathbf{w}^1 - 2\Delta t \mathbf{g}^0, \tag{30}$$

where $\mathbf{g}^0 = \{g(x_1), g(x_2), \ldots, g(x_{n-1})\}^{\mathrm{T}}$. Using Eq. (30) a system of Eqs. (29) can be rewritten as a set of two systems of equations:

$$\begin{cases} (\mathbf{A}_M - \mathbf{A}_C)\mathbf{w}^1 = \mathbf{A}_K \mathbf{w}^0 - 2\Delta t \mathbf{A}_C \mathbf{g}^0 + \mathbf{f}^0, \\ \mathbf{A}_M \mathbf{w}^{k+1} = \mathbf{A}_K \mathbf{w}^k + \mathbf{A}_C \mathbf{w}^{k-1} + \mathbf{f}^k, \quad k = 1, 2, \ldots . \end{cases} \tag{31}$$

The central finite difference (CEFD) will from now on be the notation where the initial boundary-value problem (1)–(4) is solved using the central difference method.

5. Numerical studies

In this section a few numerical examples are presented to demonstrate the effect of various parameters on the dynamic response of the axially moving belt obtained by three approximate methods and to validate the presented GFEN method. In all the numerical cases the initial conditions regarding Eq. (1) will be expressed as

$$h(x) = 0\,\mathrm{m}, \quad g(x) = 0\,\mathrm{m/s}, \quad t = 0\,\mathrm{s}. \tag{32}$$

A zero distributed load is assumed. The functions of the generalized support excitations are given in the form

$$\delta_1(t) = 0\,\mathrm{m} \quad \delta_2(t) = 0.04(1 - \cos(20\pi t))\,\mathrm{m}, \quad 0\,\mathrm{s} \leqslant t \leqslant t_k. \tag{33}$$

The other beam (belt) parameters are given in Table 1. The dynamic responses obtained using the GFEN, GN and CEFD methods are compared for various bending stiffnesses and different belt velocities. In order to compare the time histories obtained with all three methods, the estimated error of the dynamic response should be less than $10^{-4}L$ of the true value for all the velocities and bending stiffnesses in our numerical studies. Since the Newmark method is unconditionally stable, no spurious oscillations arise in the solution obtained using the GFEN and GN methods. The convergence of the GFEN and GN methods is rapid. In order to ensure the prescribed accuracy in the case of the GFEN method the spatial discretization step should be at least 1.25×10^{-2} m. In the case of the GN method, by taking at least 50 terms ($N = 50$) in the series solution, Eq. (24), the prescribed accuracy is ensured. The time-discretization step in both methods should be at least $\Delta t = 0.0001$ s. In contrast, the CEFD method is an explicit, conditionally stable scheme. In order to ensure stability the time-discretization step should be arbitrarily small, according to the chosen space-discretization step. The convergence of the CEFD method is relatively slow. To ensure the prescribed accuracy and stability the space- and time-discretization steps should be

Table 1
Beam parameters

L (m)	m (kg/m)	T (N)
1	0.1	80

chosen at least $h = 1.25 \times 10^{-2}$ m and $\Delta t = 5 \times 10^{-6}$ s. It is obvious that the computational time of the CEFD method is much greater than the computational time of the GFEN and GN methods. Although the CEFD method is the simplest one, it is relatively time consuming. By increasing the a/c ratio the convergence of all three methods is faster; however, by increasing the velocity the convergence of the methods becomes slower. Thus, in our case choosing space- and time-discretization steps $h = 1.25 \times 10^{-2}$ m and $\Delta t = 5 \times 10^{-6}$ s the prescribed accuracy for all three methods is achieved.

5.1. Undamped string model analysis: $a/c = 0$ m, $d = 0$ Ns/m

In the following analysis the bending stiffness and damping contributions are neglected: $a/c = 0$ m and $d = 0$ Ns/m. Thus, the belt is modeled as an axially moving undamped string. In this special case the results obtained with the presented approximate methods can readily be compared with the exact solutions given in Ref. [17]. In Table 2 the comparison of approximate solutions with the exact solution and the relative error estimate are given at the position $x = 0.625L$. The results obtained with the GFEN and CEFD methods are in good agreement with the exact values for all the axial velocities. It can also be seen that the results obtained with the GN method are in good agreement with the exact solution at zero axial velocity, $v = 0$ m/s. However, as the velocity increases the results obtain with the GN method do not converge to the exact values.

5.2. String model analysis: $a/c = 0$ m, $d = 0.5$ Ns/m

Assume that the bending stiffness of the belt is neglected, $a/c = 0$ m. Thus, the belt is modeled as an axially moving string. The dynamic deflection of the axially moving string is calculated using all three methods and making a comparison at the position $x = 0.625L$. In order to show the influence of the velocity on the method of the solution, dynamic deflections are calculated at four different velocities. In Fig. 4 the time histories obtained with the GFEN, GN and CEFD methods at different velocities are presented. The results indicate that in the case when the velocity is equal to zero (Fig. 4(a)) there is practically no difference between the two dashed lines and the one solid line. As the velocity increases the difference between the two dashed lines and the one solid line increases, as can be seen in Figs. 4(b)–(d). The dashed–dot line obtained with the GFEN method and the dashed line obtained with the CEFD method are overlapping, which indicates that the GFEN and CEFD methods give practically the same results. It can be seen that by increasing the relative axial velocity v/c the results obtained with the GN method do not converge to the same values obtained with the GFEN and CEFD methods.

Table 2
Comparison of approximate solutions with the exact solutions

Time (s)	Exact solution (m)	GFEN		CEFD		GN	
		Solution (m)	Error (%)	Solution (m)	Error (%)	Solution (m)	Error (%)
$v/c = 0$							
0.1	−0.043967	−0.043969	0.0059	−0.043971	0.0105	−0.043969	0.0060
0.2	−0.013681	−0.013676	0.0346	−0.013797	0.8473	−0.013676	0.0344
0.3	−0.024855	−0.024861	0.0211	−0.024859	0.0138	−0.024861	0.0214
0.4	−0.037963	−0.037958	0.0114	−0.037990	0.0720	−0.037959	0.0109
$v/c = 0.35$							
0.1	−0.021042	−0.021060	0.0828	−0.021043	0.0009	−0.016152	23.2421
0.2	−0.077976	−0.077992	0.0203	−0.077977	0.0008	−0.066207	15.0926
0.3	−0.068971	−0.068970	0.0016	−0.068974	0.0034	−0.067494	2.1415
0.4	−0.008036	−0.008034	0.0364	−0.008040	0.0424	−0.008142	1.3147
$v/c = 0.53$							
0.1	0.039996	0.039977	0.0478	0.039992	0.0095	0.045472	13.6902
0.2	0.073357	0.073318	0.0537	0.073344	0.0176	0.086105	17.3779
0.3	0.099738	0.099677	0.0610	0.099706	0.0320	0.121426	21.7449
0.4	0.118865	0.118782	0.0697	0.118812	0.0449	0.151058	27.0836

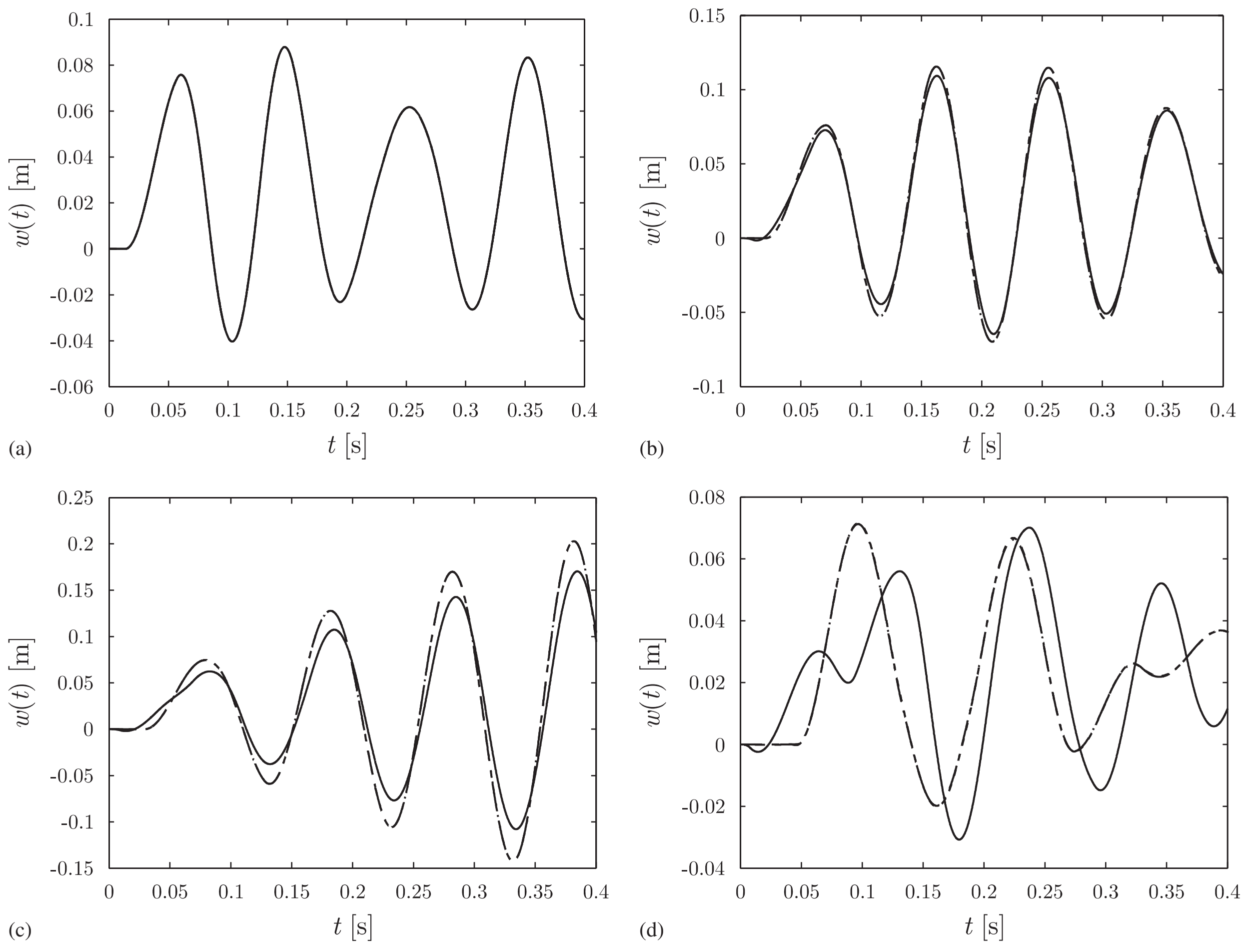

Fig. 4. Dynamic response of the axial moving string obtained at position $x = 0.625\,L$: (a) relative axial velocity $v/c = 0$; (b) relative axial velocity $v/c = 0.35$; (c) relative axial velocity $v/c = 0.53$; (d) relative axial velocity $v/c = 0.71$. (– · –) GFEN method, (——) GN method, (– – –) CEFD method.

5.3. Beam model analysis: $a/c = 0.3\,\mathrm{m}$, $d = 0.5\,\mathrm{Ns/m}$

In the following analysis the bending stiffness is taken into account, $a/c = 0.3\,\mathrm{m}$. Thus, the belt is modeled as an axially moving beam. The dynamic deflections obtained with the CEFD, GFEN and GN methods are compared at the same position as in the string case, $x = 0.625L$. Fig. 5 indicates that at high velocities the results obtained with all three methods agree very well. It can be shown that at low velocities the differences between the results obtained with all three method are even smaller. If we compare the time histories of the string and the beam at the same velocity it is obvious that the difference between the solution obtained with the GN method and the solutions obtained with the GFEN and CEFD methods is larger in the string case.

In Fig. 6 the mean relative difference between the dynamic responses obtained with the GFEN and GN methods is shown as a function of the axial velocity and the bending stiffness. The mean relative difference is calculated using the following equation:

$$\varepsilon(v) = \frac{1}{n_p L}\left|(w_{\mathrm{GFEN},v}(x,t) - w_{\mathrm{GN},v}(x,t))\right|, \quad 0 \leqslant v \leqslant 0.53c, \quad x = 0.625L, \tag{34}$$

where $w_{\mathrm{GFEN},v}(x,t)$ and $w_{\mathrm{GN},v_i}(x,t)$ denote the dynamic responses obtained with the GFEN and GN methods at an axial velocity v and at position $x = 0.625\,\mathrm{m}$. The variable n_p denotes the number of all the points in the dynamic response. It is clear from Fig. 6 that if the axial velocity increases the mean relative difference ε

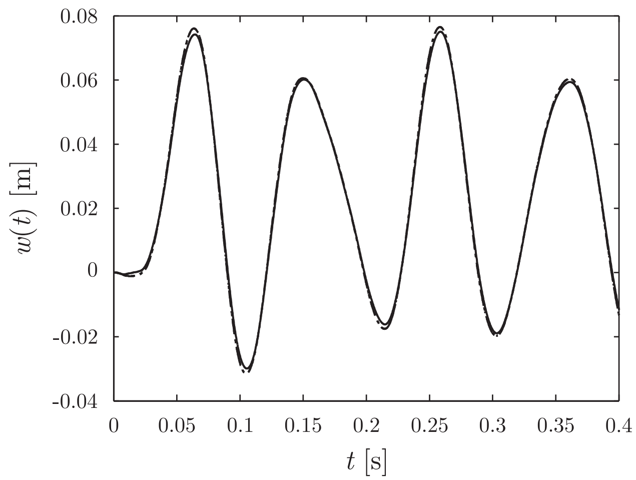

Fig. 5. Dynamic response of the axially moving beam obtained at position $x = 0.625\,L$ and relative axial velocity $v/c = 0.71$. (– · –) GFEN method, (——) GN method, (– – –) CEFD method.

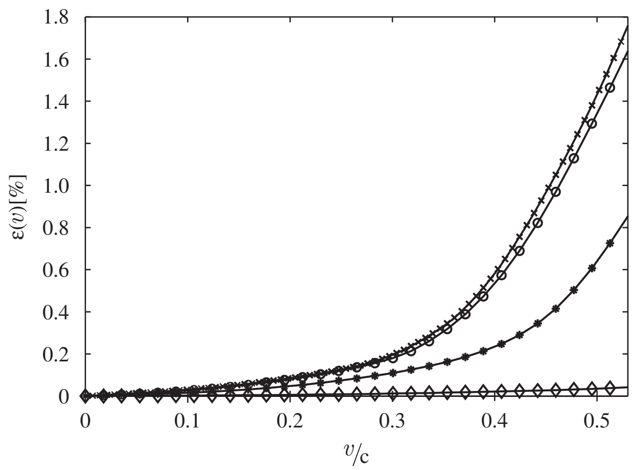

Fig. 6. Mean relative difference $\varepsilon(v)$ versus relative axial velocity for different values of relative bending stiffness at position $L = 0.625$ m. ($-\times-$) $a/c = 0$ m, ($-\circ-$) $a/c = 0.03$ m, ($-*-$) $a/c = 0.1$ m, ($-\diamond-$) $a/c = 0.3$ m.

increases exponentially. On the other hand, when the relative bending stiffness a/c is increased the mean absolute difference ε is reduced.

6. Conclusion

In this paper the transverse oscillations in a traveling beam due to the arbitrary lateral vibrations of the support(s) have been studied. It has been shown how the dynamic response of the initial boundary-value problem that describes these oscillations can be obtained using an approximate Galerkin finite-element method and the Newmark method. The presented method enables us to include the dissipation of energy in the form of an equivalent viscous-damping model. So, in this paper the solution method that combines the arbitrary support excitations and the damping mechanism was presented.

In order to verify the presented Galerkin finite-element method a quantitative comparison between three approximate methods was preformed. The results obtained with all three approximate methods were first compared with the exact solution for the case of the undamped traveling string. Subsequently, when the exact solution was not available, only the comparison between the approximate solution was preformed. Based on this comparison a new phenomenon regarding the Galerkin method was observed. Our case study shows that the Galerkin–Newmark method seems to give a poor prediction of the dynamic response for certain parameters of the system. Numerical studies indicate that the velocity and the bending stiffness appear to have a significant effect on the difference between the dynamic response obtained with the Galerkin-finite-element-Newmark and the Galerkin–Newmark methods. The mean relative difference $\varepsilon(v)$ increases exponentially with the axial velocity and decreases with the bending stiffness. Considering a comparison of the approximate solutions with the exact solution and from the fact that two different methods, the Galerkin-finite-element-Newmark and the finite-difference, give practically the same results for various parameters of the system, one can assume that at high velocities the Galerkin–Newmark method gives a poor prediction of the dynamic response.

From the above-mentioned observations one can conclude that the problem lies in the spatial discretization and not in the time discretization of the Galerkin–Newmark method. So, the Galerkin method, where stationary string eigenfunctions are used, should be used carefully when applied to the spatial discretization of axially moving continua. On the other hand, the presented Galerkin finite-element method seems to be suitable for the spatial discretization of axial moving continua for various parameters of the system.

Appendix A

In this appendix the elements of the mass $\mathbf{M_e}$, damping $\mathbf{C_e}$ and stiffness $\mathbf{K_e}$ matrices of the finite element are presented:

$$\mathbf{M_e} = h\begin{bmatrix} \frac{13}{35} & \frac{11h}{210} & \frac{9}{70} & -\frac{13h}{420} \\ \frac{11h}{210} & \frac{h^2}{105} & \frac{13h}{420} & -\frac{h^2}{140} \\ \frac{9}{70} & \frac{13h}{420} & \frac{13}{35} & -\frac{11}{210}h \\ -\frac{13}{420}h & -\frac{h^2}{140} & -\frac{11h}{210} & \frac{h^2}{105} \end{bmatrix},$$

$$\mathbf{C_e} = \begin{bmatrix} -v+\frac{13hE}{35} & \frac{hC}{10}+\frac{11h^2b}{210} & v+\frac{9hE}{70} & -\frac{hC}{10}-\frac{13h^2b}{420} \\ -\frac{hC}{10}+\frac{11h^2b}{210} & \frac{h^3b}{105} & \frac{hC}{10}+\frac{13h^2b}{420} & -\frac{h^2v}{30}-\frac{h^3b}{140} \\ -v+\frac{9hE}{70} & -\frac{hC}{10}+\frac{13h^2b}{420} & v+\frac{13hb}{35} & \frac{hC}{10}-\frac{11h^2b}{210} \\ \frac{hC}{10}-\frac{13h^2b}{420} & \frac{h^2v}{30}-\frac{h^3b}{140} & -\frac{hC}{10}-\frac{11h^2b}{210} & \frac{h^3b}{105} \end{bmatrix},$$

$$\mathbf{K_e} = \begin{bmatrix} -\frac{bv}{2}+\frac{12a^2}{h^3}+\frac{6(c^2-v^2)}{5h} & \frac{11(c^2-v^2)}{10}+\frac{6a^2}{h^2}+\frac{hbv}{10} & \frac{bv}{2}-\frac{12a^2}{h^3}-\frac{6(c^2-v^2)}{5h} & \frac{(c^2-v^2)}{10}+\frac{6a^2}{h^2}-\frac{bvh}{10} \\ \frac{(c^2-v^2)}{10}+\frac{6a^2}{h^2}-\frac{hbv}{10} & \frac{4a^2}{h}+\frac{2(c^2-v^2)h}{15} & -\frac{(c^2-v^2)}{10}-\frac{6a^2}{h^2}+\frac{hbv}{10} & \frac{2a^2}{h}-\frac{h(c^2-v^2)}{30}-\frac{h^2bv}{60} \\ -\frac{bv}{2}-\frac{12a^2}{h^3}-\frac{6(c^2-v^2)}{5h} & -\frac{(c^2-v^2)}{10}-\frac{6a^2}{h^2}-\frac{hbv}{10} & \frac{bv}{2}+\frac{12a^2}{h^3}+\frac{6(c^2-v^2)}{5h} & -\frac{11(c^2-v^2)}{10}-\frac{6a^2}{h^2}+\frac{hbv}{10} \\ \frac{(c^2-v^2)}{10}+\frac{6a^2}{h^2}+\frac{hbv}{10} & \frac{2a^2}{h}-\frac{h(c^2-v^2)}{30}+\frac{h^2bv}{60} & -\frac{(c^2-v^2)}{10}-\frac{6a^2}{h^2}-\frac{hbv}{10} & \frac{4a^2}{h}+\frac{2h(c^2-v^2)}{15} \end{bmatrix}.$$

Appendix B

In this appendix the central difference approximations of the derivatives in Eq. (1) are given.

$$\frac{\partial^4 w(x_i, t_k)}{\partial x^4} \approx \frac{w_{i-2}^k - 4w_{i-1}^k + 6w_i^k - 4w_{i+1}^k + w_{i+2}^k}{h^4}, \tag{35}$$

$$\frac{\partial^2 w(x_i, t_k)}{\partial x^2} \approx \frac{w_{i-1}^k - 2w_i^k + w_{i+1}^k}{h^2}, \tag{36}$$

$$\frac{\partial^2 w(x_i, t_k)}{\partial x \, \partial t} \approx \frac{w_{i-1}^{k-1} - w_{i-1}^{k+1} - w_{i+1}^{k-1} + w_{i+1}^{k+1}}{4h\Delta t}, \tag{37}$$

$$\frac{\partial^2 w(x_i, t_k)}{\partial t^2} \approx \frac{w_i^{k-1} - 2w_i^k + w_i^{k+1}}{\Delta t^2}, \tag{38}$$

$$\frac{\partial w(x_i, t_k)}{\partial t} \approx \frac{-w_i^{k-1} + w_i^{k+1}}{2\Delta t}, \tag{39}$$

$$\frac{\partial w(x_i, t_k)}{\partial x} \approx \frac{-w_{i-1}^k + w_{i+1}^k}{2h}. \tag{40}$$

References

[1] S. Mahalingam, Transverse vibrations of power transmission chains, *British Journal of Applied Physics* 8 (1957) 145–148.

[2] F.R. Archibald, A.G. Emslie, The vibration of a string having a uniform motion along its length, *Journal of Applied Mechanics* 25 (1958) 347–348.

[3] S. Abrate, Vibrations of belts and belt drives, *Mechanism and Machine Theory* 27 (1992) 645–659.

[4] M. Pakdemirli, A.G. Ulsoy, A. Ceranoglu, Transverse vibration of an axially accelerating string, *Journal of Sound and Vibration* 169 (1994) 179–196.

[5] H.R. Öz, M. Pakdemirli, Vibrations of an axially moving beam with time-dependent velocity, *Journal of Sound and Vibration* 227 (1999) 239–257.

[6] G. Suweken, W.T. Van Horssen, On the transversal vibrations of a conveyor belt with a low and time-varying velocity. Part I: the string-like case, *Journal of Sound and Vibration* 264 (2003) 117–133.

[7] L.Q. Chen, X.D. Yang, Stability in parametric resonance of axially moving viscoelastic beams with time-dependent speed, *Journal of Sound and Vibration* 284 (2005) 879–891.

[8] J.A. Wickert, Non-linear vibration of a traveling tensioned beam, *International Journal of Non-Linear Mechanics* 27 (1992) 503–517.

[9] F. Pellicano, F. Zirilli, Boundary layers and nonlinear vibrations in an axially moving beam, *International Journal of Non-Linear Mechanics* 33 (1998) 691–711.

[10] F. Pellicano, V. Vestroni, Nonlinear dynamics and bifurcations of an axially moving beam, *Journal of Vibration and Acoustics* 122 (2000) 21–30.

[11] H.R. Öz, M. Pakdemirli, H. Boyaci, Non-linear vibrations and stability of an axially moving beam with time-dependent velocity, *International Journal of Non-Linear Mechanics* 36 (2001) 107–115.

[12] L.Q. Chen, X.D. Yang, Steady-state response of axially moving viscoelastic beams with pulsating speed: comparison of two nonlinear models, *International Journal of Solids and Structures* 42 (2005) 37–50.

[13] A.A.N. Al-Jawi, C. Pierre, A.G. Ulsoy, Vibration localization in dual-span, axially moving beams, part I: formulation and results, *Journal of Sound and Vibration* 179 (1995) 243–266.

[14] A.A.N. Al-Jawi, C. Pierre, A.G. Ulsoy, Vibration localization in dual-span, axially moving beams, part II: perturbation analysis, *Journal of Sound and Vibration* 179 (1995) 267–287.

[15] A.A.N. Al-Jawi, A.G. Ulsoy, C. Pierre, Vibration localization in band-wheel systems: theory and experiment, *Journal of Sound and Vibration* 179 (1995) 289–312.

[16] J.A. Wickert, C.D. Mote, Classical vibration analysis of axially moving continua, *Journal of Applied Mechanics* 57 (1990) 738–744.

[17] W.T. van Horssen, On the influence of lateral vibrations of supports for an axially moving string, *Journal of Sound and Vibration* 268 (2003) 323–330.

[18] A. Pramila, J. Laukkanen, M. Pautamo, Vibration of axially moving material using the FEM, *The American Society of Mechanical Engineers* (*Paper*) (1983) 83-DET-96.

[19] N. Jakšič, M. Boltežar, Viscously damped transverse vibrations of an axially-moving string, *Journal of Mechanical Engineering* 9 (2005) 560–569.

[20] L. Lengoc, H. McCallion, Transverse vibration of a moving string: a comparison between the closed-form solution and the normal-mode solution, *Journal of Systems Engineering* 6 (1996) 72–78.
[21] F. Pellicano, G. Catellani, A. Fregolent, Parametric instability of belts: theory and experiments, *Computers and Structures* 82 (2004) 81–91.
[22] K.J. Rajesh, R.G. Parker, Spatial discretization of axially moving media vibration problems, *Journal of Vibration and Acoustics* 122 (2000) 290–294.
[23] S. Naguleswaran, C.J.H. Williams, Lateral vibration of band-saw blades, pulley belts and the like, *International Journal of Mechanical Sciences* 10 (1968) 239–250.
[24] A. Quarteroni, R. Sacco, F. Saleri, *Numerical Mathematics*, Springer, New York, 2000.